# Kinase-catalyzed biotinylation of DNA

Thilani M. Anthony[a] and Mary Kay H. Pflum[a*]

[a]Department of Chemistry, Wayne State University, 5101 Cass Avenue, Detroit, MI 48202

Abstract

Prior work documented use of γ-phosphate modified ATP analogs to label DNA using T4 polynucleotide kinases (T4PNK), although applications have been limited. To fully characterize kinase-catalyzed labeling of nucleic acids, we explored use of ATP-biotin as a cosubstrate with T4PNK. T4PNK accepted ATP-biotin to 5′-label single stranded DNA. However, T4PNK-mediated labeling of double stranded substrates was low yielding. In addition, the phosphoramidate bond connecting the biotin group to the DNA was unstable. These results suggest that kinase-catalyzed biotinylation will be useful with single stranded DNA substrates and mild reaction conditions. By revealing the scope and limitations of kinase-catalyzed biotinylation, these studies provide a foundation for future development and application of kinase-catalyzed labeling to DNA-based biological studies.

* Corresponding author. Tel.: 313-577-1515; fax: 313-577-8822; e-mail: pflum@wayne.edu

## 1. Introduction

Polynucleotide kinase (PNK) is a ubiquitous enzyme in cells that plays an important role in the repair of damaged DNA and RNA after oxidative damage,[1] ionizing radiation,[2] and base excision.[3] Damage to polynucleotides can result in genetic mutations that could lead to cell death or changes in growth. To repair DNA or RNA break points, PNK restores the appropriate 5′-phosphate and 3′-OH of the polynucldeotide to allow strand re-ligation and repair.[4]

PNK is also a commonly used reagent to phosphorylate polynucleotides in molecular biology.[5, 6] Commercially-available, recombinant T4 polynucleotide kinase (T4PNK) is used with adenosine 5′-triphosphate (ATP) to phosphorylate the 5′-end of single stranded and double stranded DNA or RNA, synthetic oligonucleotides, and nucleoside 3′-monophosphates for molecular cloning applications (Figure 1A).[7,8] Another common application of T4PNK is radiolabeling polynucleotides using [γ-$^{32}$P]ATP for use as hybridization probes for blotting, DNA/RNA sequencing, or gel shift experiments to study protein-DNA complexes. As radiolabeling requires handling hazardous materials, a non-hazardous and robust labeling technique would be a desirable alternative. In addition, a new labeling method could also have application to the study of PNK biology.

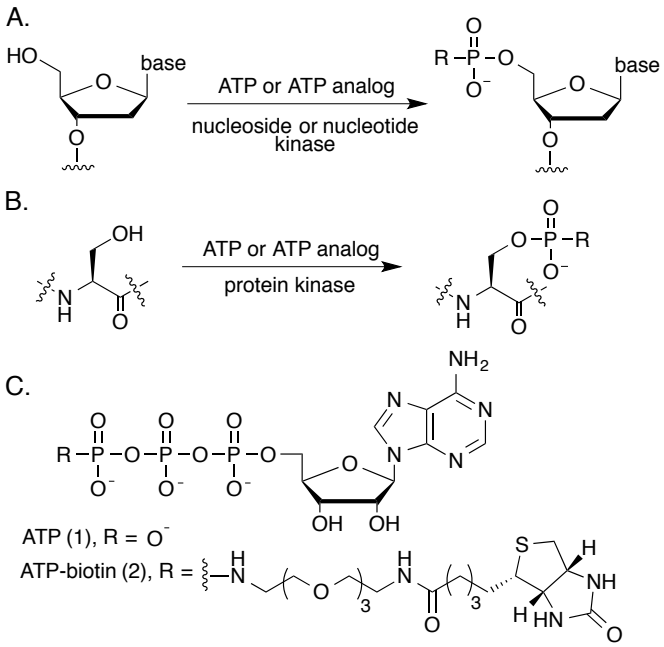


Figure 1. Reaction of a nucleotide substrate with a nucleotide kinase, such as T4PNK (A), or reaction of protein substrate with a protein kinase (B) with either ATP or a γ-phosphate-modified ATP analog (C) will produce a labeled product.

Our lab recently discovered a novel property of kinases called “kinase cosubstrate promiscuity”. By studying protein kinases, we found that γ-phosphate modified ATP analogs were compatible as cosubstrates (Figure 1B), leading to protein labeling.[9] Many different functional groups, such as biotin, dansyl, and arylazide, were linked to the γ-phosphate of ATP and were successfully transferred to the protein substrate via kinase-catalyzed labeling.[10,11-13]

Although kinase-catalyzed labeling has been used with protein substrates, application to non-protein kinases is understudied. In the case of polynucleotide kinases, γ-phosphate modified ATP analogs would 5′-label a DNA substrate (Figure 1A). T4PNK is a 301 amino acid polypeptide that forms a homotetramer.[14] Site-directed mutagenesis indicated that the T4PNK monomer contains an N-terminal 5′-kinase domain and a C-terminal 3′-phosphatase domain.[15,16] The previously reported crystal structure of the T4PNK kinase domain bound to ADP showed that the diphosphate chain is positioned near a solvent-exposed, 15–20 Å diameter central channel within the enzyme tetramer (Figure 2).[17] Given the likely solvent exposure of the kinase domain near the γ-phosphate of ATP, the crystal structural analysis suggests that T4PNK could accommodate the binding of a bulky γ-phosphate modified ATP analog for kinase-catalyzed labeling.

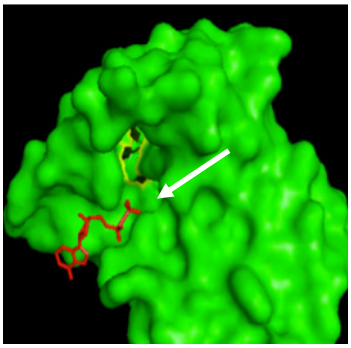

Figure 2. T4 nucleotide kinase (green) in complex with ADP (red) and nucleotide substrate (yellow) (PDB: 1RRC). ADP is bound to the solvent-exposed surface of T4PNK, as indicated by the white arrow.

Consistent with the cosubstrate promiscuity of nucleotide kinases, one report documented T4PNK-mediated thiophosphorylation with ATPγS, followed by *in situ* alkylation to introduce a biotin group onto an RNA/DNA substrate in two-steps.[18] Another study demonstrated use of ATP analogs with photocrosslinking groups to label single stranded DNA substrates.[19] Finally, a T4PNK activity assay was reported involving kinase-catalyzed biotinylation of DNA immobilized on a glass slide by T4PNK and an ATP-biotin analog (Figure 1C), followed by single-molecule, nanoparticle imaging.[20] Although several reports documented that γ-phosphate modified ATP analogs are compatible with PNK,[18-20] rigorous characterization of kinase-catalyzed labeling is lacking, which has limited its use in DNA research.

In this work, our objective was to rigorously characterize γ-phosphate modified ATP analogs as cosubstrates of T4PNK. ATP-biotin was selected due to the utility of biotinylation to both visualize and purify DNA. A variety of qualitative and quantitative data indicated that ATP-biotin acts as a cosubstrate of T4PNK, which is consistent with prior work. However, the size of the DNA substrate and the stability of the phosphoramidate-linked biotin group were key issues that govern success of the reaction. These studies provide guidance for future use of kinase-catalyzed biotinylation in DNA research.

## 2. Materials and Methods

### *2.1. Synthesis of ATP-biotin*

ATP-biotin was synthesized as previously published.[21]

### *2.2. ADP-Glo kinase assay*

In a 96-well white plate, T4PNK (2 units/μL) was mixed with 28-mer DNA (20 μM) in T4PNK buffer (1X; 0.5 mM dithiothreitol (DTT), 0.25 mM $MgCl_2$, and 7 mM Tris–HCl, pH 8.0). The kinase reaction was initiated by adding ATP or ATP-biotin (200 μM). Final volumes of the reactions were 25 μL. The reactions were incubated at 37 °C for 1 hr and then terminated by adding ADP-Glo™ reagent (25 μL) and incubating at room temperature for 40 min. Kinase detection reagent (50 μL) was added and the reaction was incubated for 30 min at room temperature. Finally, luminescence signal was measured using a microplate reader (GENios Plus, Tecan). The mean luminescence signal and standard error from three independent trials is displayed in Figure 3A and Table S1.

Kinetic studies with T4PNK was performed using ADP-Glo™ kinase assay (Promega) as described above, except with higher concentrations of 28mer substrate (50 μM) and several concentrations of ATP (1, 3, 10, 30, and 100 μM) or ATP-biotin (10, 30, 100, 300, and 1000 μM) cosubstrate. For kinetics, the reaction was initiated

by adding 28mer substrate in a final volume 20 μL. The reaction mixtures were incubated at 37 °C for 5, 10, and 15 min for each concentration. After the incubation period, an equal amount of ADP-Glo™ reagent (20 μL) was added to the mixture and incubated for 40 min at room temperature. Then, the kinase detection reagent (40 μL) was added to the reaction mixture and allowed to react for 30 min at room temperature. Finally, luminescence signal was monitored with a micro plate reader (GENios Plus, Tecan). Background correction was performed by subtracting the signal of a reaction without 28mer DNA substrate. The concentration of ADP produced was determined using a standard curve (Figure S1). The concentration of ADP generated in each reaction was plotted over the time and the initial rate of the reaction was obtained from the slope of the linear portion of the plot (Figure S2). The experimental results (rate vs. substrate concentration) were fit to the Michaelis–Menton equation ($v = V_{max}[S]/(K_M + [S])$, where $v$ = rate of the reaction and $[S]$ = substrate concentration) by non-linear regression using Kaleidagraph software (Synergy Software) to obtain $K_M^{app}$ and $V_{max}^{app}$ values (Figure S2). $V_{max}^{app}$ was divided by the concentration of enzyme (0.011 μM) to obtain the $k_{cat}^{app}$ value. Because the concentrations of DNA substrate used in each reaction were less than 10-fold above the substrate $K_M$, the $K_M$ and $k_{cat}$ values are shown as $K_M^{app}$ and $k_{cat}^{app}$. The mean and standard error was obtained from two or three independent trials (Figure 3B).

*2.3. T4PNK-catalyzed labeling reactions*

Oligomer substrate (14-mer, 28-mer, or 37-mer DNA, 20 μM) in distilled water was heated in a boiling water bath for 1 min and then immediately dipped in an ice bath. After 2 min of cooling, T4PNK buffer, ATP or ATP-biotin (200 μM), and T4PNK enzyme (2 units/μL) were added in a 50 μL total volume. The reaction was mixed well by pipetting and incubated at 37 ºC for 2 hrs without shaking. Critical controls included reactions where T4PNK or ATP-biotin was omitted. The reactions were analyzed as described below.

*2.4. MALDI-TOF mass spectrometric analysis*

After T4PNK-catalyzed labeling (section 2.3), oligomer products were purified by ethanol precipitation as follows. Sodium acetate (75 mM, pH 5.2) and ethanol (75%) were added to the kinase reaction and incubated on dry ice for 30 min. Samples were centrifuged at 14,000 x g for 30 minutes at 4 ºC to collect the DNA pellet. The product pellet was dissolved in $dH_2O$ (2 μL) and then mixed with a saturated solution of 3-hydroxypicolinic acid matrix in 1:1 acetonitrile:0.0833 M ammonium citrate in water (2 μL). The sample (1 μL) was spotted onto a MTP Plate (Bruker) and analyzed using a MALDI-TOF instrument (Bruker Ultraflex). Full spectra and repetitive trial are shown in Figures 3C and S3.

*2.5. Gel shift analysis*

Oligomer products after T4PNK-catalyzed labeling (section 2.3) were separated by 20% denaturing urea polyacrylamide gel electrophoresis in Tris/Borate/EDTA (TBE) buffer (1X: 89 mM Tris, pH 7.6, 89 mM boric acid, 2 mM EDTA) and visualized using SYBR Gold Nucleic Acid Gel Stain (Life Technologies) according to the manufacturers protocol. Oligomer gel bands from SYBR Gold Nucleic Acid Gel Stain were detected on a Typhoon imager (excitation wavelength 495 nm and an emission at 537 nm). Band intensities were quantified using ImageQuant 5.1 by drawing the same size rectangular shape around comparable bands. Conversion percentages were calculated by dividing the intensity of the product band by the intensity of the total DNA, and multiplying by 100. Repetitive trials are shown in Figures 4, S4, S5, and S6.

*2.6. Southern blot analysis*

The 37-mer DNA fragment was used as the forward primer (0.5 μM) in a 50 μL PCR reaction containing reverse primer (0.5 μM), template DNA (0.5 μM; pBJ5-HDACI)[22], dNTP (200 μM each), DMSO (10 %) and *Pfu* DNA Polymerase enzyme (0.025 units/μL) in *Pfu* DNA Polymerase buffer (20 mM Tris-HCl (pH 8.8), 10 mM KCl, 10 mM $(NH_4)_2SO_4$, 2 mM $MgSO_4$, 0.1 mg/mL nuclease-free BSA, and 0.1% Triton® X-100). After PCR amplification, the 417-mer product was purified on a 1% agarose gel in 1X TBE buffer (89 mM Tris, pH 7.6, 89 mM boric acid, 10 mM EDTA). The gel band with the correct 417 base pair size was excised and purified by QIAquick Gel Extraction Kit spin columns (Qiagen). The concentration of purified DNA was determined using UV/Vis spectroscopy. The purified PCR product was then used in a T4PNK-catalyzed biotinylation reaction (section 2.3). The T4PNK reaction product was separated using a 0.7% agarose gel in 0.5X TBE buffer (44.5 mM Tris, pH 7.6, 44.5 mM boric acid, 1 mM EDTA). A positive control PCR reaction was also included in the gel analysis, which was generated using a synthetic 5'-biotinylated 37-mer (0.5 μM) as the forward primer. The gel was soaked in the alkaline transfer buffer (0.4 N NaOH, 1 M NaCl) for 45 min, followed by capillary transfer using Immobilon-Ny+ membrane (EMD Millipore). After 8 hrs of transfer, the membrane was blocked using blocking buffer (90 mM sodium citrate, 900 mM NaCl, 0.5% SDS, 100 μg/mL salmon sperm DNA, 1 mM EDTA, pH 7.0) for 2 hrs. The membrane was then stained with SYBR Gold Nucleic Acid Gel Stain or a Streptavidin-

Cy5 conjugate according to the manufacturers protocols, followed by scanning using a Typhoon scanner (Amersham Biosciences). SA-Cy5 stained membranes were visualized using an excitation wavelength of 633 nm and an emission at 670 nm. Repetitive trials are shown in Figures 5A and S8.

*2.7. Dot-blot analysis*

Oligomer products after PCR amplification, gel purification, and T4PNK-catalyzed labeling (section 2.6) were transferred onto Immobilon-Ny+ membrane (EMD Millipore) using Bio-Dot® microfiltration apparatus (Bio-Rad) according to the manufacturers protocol. After transfer, the membrane was washed with $dH_2O$, followed by blocking, staining, and scanning as described in section 2.6. Spot intensities were quantified using ImageJ by drawing the same size circles around comparable spots on the SA-Cy5 stained gel. Percentage conversion was calculated by dividing the band intensity of the kinase-catalyzed biotinylated product by the band intensity of the PCR product generated using the synthetic 5'-biotinylated DNA, and multiplying by 100. Repetitive trials are shown in Figures 5B and S9.

## 3. Results

*3.1. ADP-Glo™ kinase assay*

To assess the tolerance of T4PNK for ATP-biotin, the ADP-Glo™ assay (Promega) was used to monitor production of the ADP byproduct of kinase-catalyzed labeling using a luminescence signal. We selected single stranded DNA substrates for these studies given that T4PNK shows highest efficiency with single-strand DNA.[23] A reaction containing single stranded 28-mer DNA substrate, T4PNK, and ATP-biotin produced a 1.5-fold increase in signal compared to reactions containing no substrate (Figure 3A, column 7 versus 8, and Table S1). A similar 1.7-fold signal increase was observed with ATP as the cosubstrate (Figure 3A, column 4 versus 5, and Table S1), although with higher luminescence signal. The high background signal observed with ATP and T4PNK in the absence of substrate (Figure 3A, column 4) was likely due to background hydrolysis of ATP to ADP by T4PNK, which was reduced with ATP-biotin due to the presence of the phosphoramidate bond (Figure 1C).[13, 24] The results indicate that T4PNK consumed ATP-biotin as a cosubstrate similar to natural ATP, which is consistent with kinase-catalyzed labeling with ATP-biotin.

To further characterize the reaction using the ADP-Glo™ assay, we performed kinetics studies with T4PNK and both ATP and ATP-biotin. The data showed that ATP-biotin maintained a higher $K_M^{app}$ value than ATP (8-fold elevated, Figure 3B), although the $k_{cat}^{app}$ value was higher for ATP-biotin than ATP (3-fold elevated, Figure 3B). Taken together, the $k_{cat}/K_M^{app}$ values indicated that ATP-biotin was 2.5-fold less efficient than ATP (Figure 3B). The kinetics data is consistent with end point assay (Figure 3A) indicating that T4PNK accepts ATP-biotin, albeit with lower efficiency.

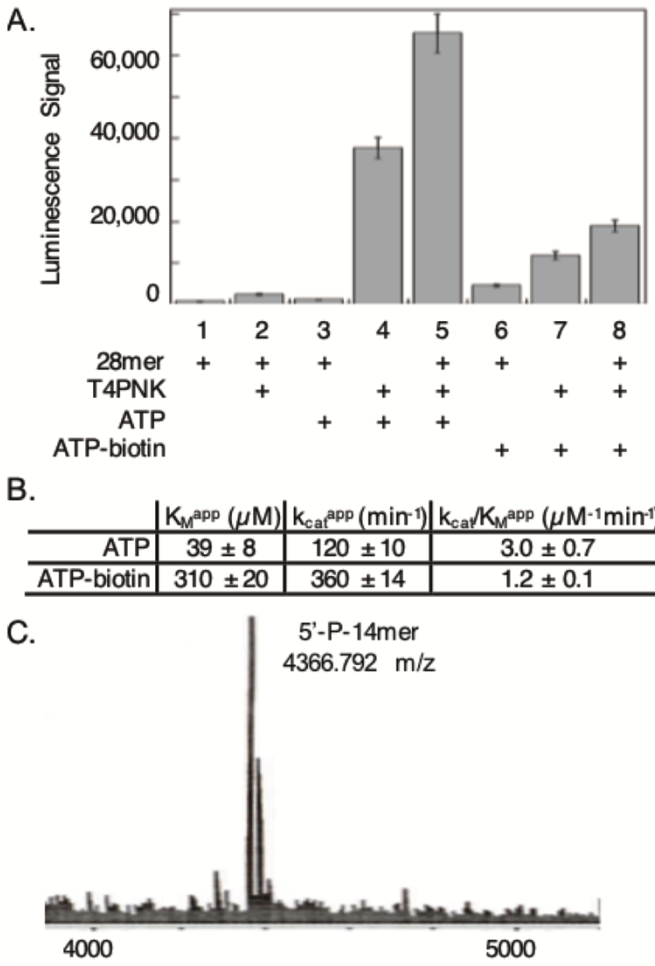


| | $K_M^{app}$ ($\mu$M) | $k_{cat}^{app}$ ($min^{-1}$) | $k_{cat}/K_M^{app}$ ($\mu M^{-1}min^{-1}$) |
|---|---|---|---|
| ATP | 39 ± 8 | 120 ± 10 | 3.0 ± 0.7 |
| ATP-biotin | 310 ± 20 | 360 ± 14 | 1.2 ± 0.1 |

igure 3. A) ADP-Glo™ assay with 28mer DNA (5′-ACCGTAGGCAAGAGTGTGCTTTTTTTTT-3′), 4PNK, and either ATP or ATP-biotin, with arbitrary luminescence units after a 30 min reaction. omponents of each reaction are indicated below each column. The data represent the mean and standard ror of three independent trials (Table S1). B) Kinetics values obtained with T4PNK and either ATP or TP-biotin using the ADP-Glo™ assay. The data are from two to three independent trials (Figures S1-2). C) MALDI-TOF MS analysis of T4PNK catalyzed 5'-biotinylation of a 14mer single stranded DNA 5′-GGGTGGCCTTGTCC- 3′) in negative ion mode. 5'-P-14mer: calculated [M-H]— 4366.9 m/z, bserved 4366.792 m/z; 5'-P-biotin-14mer calculated [M-H]—: 4795.2 m/z; not observed. For full MS pectrum see Figure S3.

*3.2. M*

To confirm kinase-catalyzed labeling occurred with T4PNK and ATP-biotin, mass spectrometry (MS) analysis was performed. A single stranded 14-mer DNA was incubated with ATP-biotin and T4PNK before separation of the DNA product from reaction components by ethanol precipitation and analysis by matrix-assisted laser desorption/ionization – time of flight (MALDI-TOF) mass spectrometry.[25] A 5′-phosphorylated 14-mer was observed (Figure 3C), which suggests that the phosphoramidate bond of the biotinylated DNA product was cleaved (Figure S10) either during the ethanol precipitation step or ionization in the mass spectrometer. The MS data provide evidence that ATP-biotin is a cosubstrate of T4PNK, consistent with the ADP-Glo™ data. However, the data also indicate that the phosphoramidate bond connecting biotin to the DNA is unstable.

*3.3. Quantitative gel shift study*

With evidence that ATP-biotin is a T4PNK cosubstrate, the reaction conversion was quantified using gel methods. Single stranded 28-mer DNA substrate was incubated with ATP-biotin and T4PNK to generate labeled DNA product. Gel analysis showed a slower migrating product after kinase-catalyzed biotinylation (Figure 4A, lane 7). The ATP-containing reaction also formed a similar slower migrating product (Figure 4A, lane 6). To assess the extent of reaction conversion, the band intensities of product versus unreacted substrate were quantified for three independent trials (Figure S4). Reaction conversions were similar with ATP (49 ± 3%) and ATP-biotin (40 ± 2%), suggesting that T4PNK accepts both cosubstrates. A slower migrating product band was absent in a

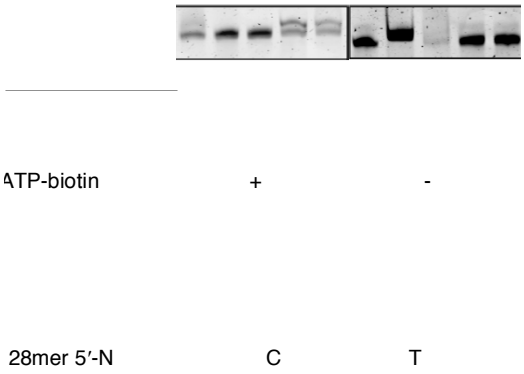


Figure 4. (A) Kinase-catalyzed biotinylation of a 28mer or 37-mer substrate with the contents of each reaction shown. Additional trials shown in Figures S2 and S3. (B) Kinase-catalyzed biotinylation of 5′-N 28-mer (where N is indicated, 5′-NAC CGT AGG CAA GAG TGT GCT TTT TTT TT-3′). The DNA was visualized with SYBR Gold (Invitrogen). Additional trials shown in Figure S4. In both A and B, a synthetic 28mer containing a 5′-biotin group (Figure S5) was included for comparison (biotin-DNA).

control conversion substrates 17 to 30 bases in length.[26] Similar conversion results were also obtained using a single stranded 37-mer DNA substrate (Figure 4A, lanes 13 and 14, and Figure S5), showing equivalent reaction conversions with ATP (47 ± 1%) and ATP-biotin (42 ± 1%). The similar results observed with both 28-mer and 37-mer substrates indicate that DNA length does not significantly affect kinase reaction.

To assess whether the 5′-base of the DNA substrate influences biotinylation, the 28-mer DNA with C, A, T or G at the 5′-position were reacted with ATP-biotin (Figure 4B). Previous studies on the efficiency of 5′-labeling with [γ-$^{32}$P]ATP and T4PNK showed highest efficiency with G as the 5′-base and lowest conversion when C is the 5′-base.[26] The electrophoresis analysis with ATP as the cosubstrate showed highest conversions with C and T, with 53 ± 5 % for 5′-A, 67 ± 4 % with 5′-C, 62 ± 10 % with 5′-T, and 47 ± 1% for 5′-G (Figure 4B and Figure S6). Compared to ATP, ATP-biotin reactions exhibited preference for 5'-C labeling, with 44 ± 16 % for 5′-A, 60 ± 3 % with 5′-C, 48 ± 8 % with 5′-T, and 43 ± 1% for 5′-G (Figure 4B and Figure S6). With ATP-biotin, the results are in contrast to an earlier report of ATP-biotin labeling with T4PNK showing highest conversions with 5′-G DNA.[20] However, these results demonstrate that the ATP-biotin reaction is compatible with DNA substrates containing all four bases at the 5′-position, with a small preference for a 5′-T.

*3.4. Southern transfer and Dot blot analyses*

To further assess T4PNK-catalyzed biotinylation, Southern and dot blot analyses were performed after ATP-biotin labeling. For Southern blot analysis, a DNA fragment appropriately sized for membrane transfer (greater than 75 bases) was first generated by polymerase chain reaction (PCR). The resulting 417-mer DNA fragment was subjected to T4PNK-catalyzed biotinylation. The 5′-biotinylated DNA product was separated by agarose gel electrophoresis, transferred to a nylon+ membrane, and then stained with either SYBR gold to visualize total DNA or a streptavidin-Cy5 conjugate to observe biotinylation. Although the SYBR gold stained membrane showed successful transfer of the amplified DNA to the membrane (Figure 5A and S6, top gel), SA-Cy5 visualized only a positive control (Figure 5A, lane 1 and Figure S8, lane 2) where a synthetic primer containing a 5′-biotin group (Figure S7) was used as the PCR primer. The ATP-biotin labeled DNA fragment was insensitive to SA-Cy5 detection (Figure 5A, lane 5). We also note that alkaline (NaOH) or neutral (pH 7) transfer conditions produced the same result.

To avoid the gel separation and transfer, which could contribute to cleavage of the phosphoramidate bond and loss of biotin (Figure S10) in the Southern blot experiment, a dot blot assay was perform. In this case, after PCR amplification and kinase-catalyzed labeling, the 5′-biotinylated DNA fragment was directly immobilized on the Nylon+ membrane using a Bio-Dot® microfiltration apparatus. SYBR gold staining confirmed successful blotting of DNA on the membrane (Figure 5B and S7A, top gel). SA-Cy5 staining showed low intensity signal from the

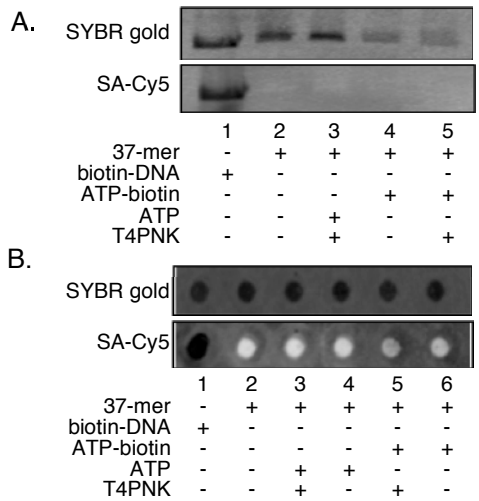


Figure 5. Southern blot (A) or dot blot (B) analysis of the 417-mer PCR amplified product generated using a 37-mer primer that was subsequently reacted with the components indicated below the lane. Total DNA was visualized by SYBR gold stain and biotin-modified DNA was visualized using a streptavidin-Cy5 (SA-Cy5) conjugate. Repetitive trials shown in Figures S6 and S7.

ATP-biotin modified DNA fragment (Figure 5B, lane 5 and Figure S9A, lane 4), with 11 ± 1 % conversion compared to the positive control reaction (Figure 5B, lane 1 and Figure S9A, lane 6, Figure S9B). While the dot blot assay showed the presence of 5′-biotinylated product, the lower efficiency compared to earlier gel analysis (42% conversion) suggested that there are limitations to T4PNK-catalyzed biotinylation.

## 4. Discussion

In this work, T4PNK-catalyzed biotinylation of DNA with ATP-biotin was rigorously tested. Prior work reported the compatibility of γ-phosphate modified ATP analogs with T4PNK.[18-20] The 5′-tagging of DNA using γ-phosphate modified ATP analogs and T4PNK could represent a useful method to facilitate the purification, visualization, and immobilization of DNA for a variety of applications. However, the limited use of kinase-catalyzed labeling in the literature suggested that the reaction needed further characterization and development.

We employed a variety of methods to characterize kinase-catalyzed biotinylation of DNA. All data confirmed the compatibility of ATP-biotin as a T4PNK cosubstrate. ADP-Glo™, gel electrophoresis, and MS analyses were consistent with labeling by ATP-biotin and T4PNK. Quantitative gel analysis showed that the ATP-biotin reaction had comparable efficiency to the ATP reaction (67-47% versus 60-40% conversions, Figures 4, S4, S5, and S6). Importantly, dot blot analyses documented the production of a biotinylated DNA product (Figures 5B and S9). Taken together, the combined data show that ATP-biotin is a T4PNK cosubstrate with conversion efficiencies comparable to ATP phosphorylation, which is consistent with prior reports.[18-20]

While the data are consistent with kinase-catalyzed biotinylation, the data also suggested several limitations of the labeling strategy. Dot blot analysis documented the presence of only 11% biotinylated DNA product after kinase-catalyzed biotinylation (Figure 5B and S9), which is significantly lower than the 42% conversions observed by gel analysis (Figures 4A and S5). Similarly, Southern blot analysis was unable to detect the presence of biotin on a PCR-generated 417-mer DNA fragment biotinylated using T4PNK and ATP-biotin (Figures 5A and S8). Finally, mass spectrometry studies only observed a 5′-phosphorylated DNA product due to cleavage of the phosphoramidate bond connecting biotin to the DNA (Figure 3C and S3).

One hypothesis explaining the low quantities of biotinylation observed in these studies is that ATP-biotin is degrading to ATP prior to kinase reaction (Figure S11A). The fact is that the phosphoramidate bond connecting the biotin group to the 5′-phosphoryl in ATP-biotin is prone to hydrolysis at low pH.[13, 27, 28] To exclude the possibility that the ATP-biotin was degrading to ATP prior to kinase-catalyzed reaction, ATP-biotin was monitored by thin layer chromatography after incubation with T4PNK in kinase buffer. No degradation was observed (Figure S11B). While ATP-biotin will hydrolyze at low pH,[28] the neutral pH conditions of the kinase buffer and binding to T4PNK did not result in significant degradation.

Another plausible hypothesis explaining the low quantities of biotinylation is that the product of kinase-catalyzed biotinylation is unstable. In this scenario, the phosphoramidate bond connecting biotin to the 5′-

phosphoryl of DNA cleaves after kinase-catalyzed biotinylation, which releases the biotin tag to generate a 5′-phosphorylated DNA product (Figure S10). This second hypothesis is consistent with the conversions seen in ADP-Glo and gel shift assays (Figure 3A, 3B, and 4), yet the minimal or absent biotin signal in the MALDI-TOF, dot blot, and Southern blot studies (Figures 3C and 5). This hypothesis suggests that efficient kinase-catalyzed biotinylation by T4PNK requires mild manipulations that avoid cleavage of the phosphoramidate bond. To overcome the stability limitations of phosphoramidate-linked ATP-biotin, ATP analogs containing phosphodiester or phosphonate bonds could be explored to create more stable labeled DNA products.[28] In fact, phosphorothioate-containing ATP analogs are cosubstrates for T4PNK and produced stable DNA products.[18]

A second reasonable hypothesis explaining the low quantities of biotinylation is that T4PNK is inefficient with ATP-biotin. Prior work documented that T4PNK and ATP phosphorylate single stranded DNA efficiently, but show a 1,000-fold loss in efficiency with double stranded DNA.[23] In this scenario, ATP-biotin and T4PNK label its preferred single stranded DNA substrate successfully, consistent with ADP-Glo and gel shift assays (Figure 3A, 3B, and 4). However, large double-stranded substrates were labeled too inefficiently with ATP-biotin to allow biotin detection, which is consistent with dot blot and Southern blot analyses (Figure 5). This hypothesis suggests that efficient kinase-catalyzed biotinylation by T4PNK is restricted to single stranded DNA substrates. Two prior reports documented kinase-catalyzed labeling of DNA using ATP analogs where the γ-phosphate group was attached via a phosphoramidate bond.[19, 20] Both reports studied T4PNK-catalyzed labeling using single stranded substrates.[19, 20] The success of earlier studies is consistent with the hypothesis that single stranded DNA substrates are required for efficient T4PNK-mediated biotinylation.

## 5. Conclusions

The ability to 5′-label DNA using kinase-catalyzed labeling has exciting potential in DNA research. The studies here confirm that T4PNK accepts the γ-modified ATP analog ATP-biotin as a cosubstrate. However, the limitations of the reaction include use of single stranded DNA substrates for high efficiency labeling and mild conditions to maintain the stability of the phosphoramidate bond connecting the biotin group to DNA. By exploring the scope and limitations of kinase-catalyzed biotinylation, these studies provide guidance for the development and application of kinase-catalyzed labeling to DNA research.

## Acknowledgments

We thank the National Science Foundation (1306493) and Wayne State University for funding, and J. Woodard for technical support.

## References and notes

1. C. Breslin, K.W. Caldecott *Mol Cell Biol* 2009, *29*, 4653-4662.
2. A. Rasouli-Nia, F. Karimi-Busheri, M. Weinfeld *Proc Natl Acad Sci U S A* 2004, *101*, 6905-6910.
3. L. Wiederhold, J.B. Leppard, P. Kedar, F. Karimi-Busheri, A. Rasouli-Nia, M. Weinfeld, A.E. Tomkinson, T. Izumi, R. Prasad, S.H. Wilson, S. Mitra, T.K. Hazra *Mol Cell* 2004, *15*, 209-220.
4. F. Karimi-Busheri, J. Lee, A.E. Tomkinson, M. Weinfeld *Nuc. Acids Res.* 1998, *26*, 4395-4400.
5. L.K. Wang, C.D. Lima, S. Shuman *The EMBO Journal* 2002, *21*, 3873-3880.
6. C.C. Richardson *Proc. Nal Acad. Sci.* USA 1965, *54*, 158-165.
7. E.J. Wood *Biochem. Educ.* 1993, *21*, 221-221.
8. G.M. Dolganov, A.V. Chestukhin, M.F. Shemyakin *Eur J Biochem* 1981, *114*, 247-254.
9. K.D. Green, M.K. Pflum *J Am Chem Soc* 2007, *129*, 10-11.
10. K.D. Green, M.K.H. Pflum *ChemBioChem* 2009, *10*, 234-237.
11. S. Garre, C. Senevirathne, M.K. Pflum *Bioorg Med Chem* 2014, *22*, 1620-1625.
12. S. Suwal, M.H. Pflum *Angew Chem Int Ed Engl* 2010, *49*, 1627-1630.
13. C. Senevirathne, D.M. Embogama, T.M. Anthony, A.E. Fouda, M.K.H. Pflum *Bioorg Med Chem* 2016, *24*, 12-19
14. L.K. Wang, S. Shuman *J.Biol. Chem.,* 2001, *276*, 26868-26874.
15. D.A. Soltis, O.C. Uhlenbeck *J. Biol. Chem.* 1982, *257*, 11340-11345.
16. E.A. Galburt, J. Pelletier, G. Wilson, B.L. Stoddard *Structure* 2002, *10*, 1249-1260.
17. K.W. Caldecott *Structure* 2002, *10*, 1151-1152.
18. G.P. Grant, P.Z. Qin *Nucleic Acids Res* 2007, *35*, e77.
19. I.O. Petrousseva, I.V. Safronov, N.I. Komarova, T.P. Kamynina, O.I. Lavrik, S.N. Khodyreva *Doklady Biochemistry and Biophysics* 2003, *389*, 114-117.
20. E.S. Yeung, C.B. Ma *Anal Bioanal Chem* 2010, *397*, 2279-2284.

21. C. Senevirathne, M.K. Pflum *ChemBioChem* 2013, *14*, 381-387.
22. M.K. Wambua, D.A. Nalawansha, A.T. Negmeldin, M.K. Pflum *Journal of medicinal chemistry* 2014, *57*, 642-650.
23. J.R. Lillehaug, R.K. Kleppe, K. Kleppe *Biochemistry* 1976, *15*, 1858-1865.
24. C. Senevirathne, K.D. Green, M.K.H. Pflum, Kinase-Catalyzed Biotinylation of Peptides, Proteins, and Lysates, Current Protocols in Chemical Biology, John Wiley & Sons, Inc.2012.
25. I.G. Gut *Human Mutation* 2004, *23*, 437-441.
26. V. van Houten, F. Denkers, M. van Dijk, M. van den Brekel, R. Brakenhoff *Anal. Biochem.* 1998, *265*, 386-389.
27. K.D. Green, M.H. Pflum *J. Am. Chem. Soc.* 2007, *129*, 10-11.
28. S.M. Hacker, M. Mex, A. Marx *J Org Chem* 2012, *77*, 10450-10454.

Supplementary Material
Supplementary material is provided with additional materials and methods, raw data for the ADP-Glo assay, repetitive trials of all experiments, and additional supporting data and figures.